Acute slice preparation

Male Wistar rats (16–31 days old; mean±SD: 27±3.7 days) were anesthetized with ketamine (50 mg per animal) in accordance with the ethical guidelines of the Institute of Experimental Medicine, Hungarian Academy of Sciences. After decapitation, the brain was removed and placed into ice-cold artificial cerebro-spinal fluid (ACSF) containing (in mM): 230 sucrose, 2.5 KCl, 25 glucose, 1.25 NaH_2PO_4, 24 $NaHCO_3$, 4 $MgCl_2$, and 0.5 $CaCl_2$. Horizontal slices from the olfactory bulb were cut at 300 μm thickness with a Vibratome (Leica VT1000S) and were stored at 33-35 °C in ACSF containing (in mM): 85 NaCl, 75 sucrose, 2.5 KCl, 25 glucose, 1.25 NaH_2PO_4, 24 $NaHCO_3$, 4 $MgCl_2$, and 0.5 $CaCl_2$. After 30 minutes, this medium was gradually replaced by or the slices were transferred to 33-35°C normal ACSF containing (in mM): 126 NaCl, 2.5 KCl, 25 glucose, 1.25 NaH_2PO_4, 24 $NaHCO_3$, 2 $MgCl_2$, and 2 $CaCl_2$ (Antal *et al.*, Eur J Neurosci, 2006, 24, 1124); and cooled to room temperature. Slices were incubated at room temperature until they were transferred to the recording chamber. All extracellular solutions were bubbled continuously with 95% O_2 and 5% CO_2, resulting in a pH of ~7.4.

Electrophysiological recordings

Cell-attached and somatic whole-cell voltage recordings were performed at 33-34°C using an identical protocol to that described previously (Antal *et al.*, Eur J Neurosci, 2006, 24, 1124). Briefly, cells were identified with an oblique illumination technique using an Olympus BX50WI microscope and a 40x water immersion objective. Recordings were carried out from the somata of juxtaglomerular cells with a diameter of <10 μm. Action potentials were evoked by injecting 1-second-long depolarizing current pulses of different amplitudes (5-70 pA). The passive properties were derived from single exponentials fitted to traces of membrane voltage responses to small (2-20 pA, 400-1000 ms) hyper- and depolarizing current injections. Data were digitized on-line at 20 kHz,

and analyzed with EVAN 1.3 and with an in-house analysis software (SPIN 1.0.1.) written in Matlab (Matlab 7.0, The MathWorks Inc., Natick, MA).

Visualization of biocytin filled cells

After the recordings, slices were placed in a fixative containing 4% PFA, 0.05%-1.25% GA and 15 v/v% picric acid in 0.1 M PB at 4ºC and the biocytin was visualized according to the protocol described previously (Antal *et al.*, Eur J Neurosci, 2006, 24, 1124). Immunofluorescent labeling for CR and Kv4.3 subunit was performed on 11 out of the 47 slices as described above.

Ultrastructural identification of mitral and granule cell dendrites and external tufted cell and periglomerular cell somata

In our study, the same criteria for distinguishing mitral and granule cell dendrites were used as in Peters, Palay and Webster, The Fine Structure of the Nervous System (Oxford University Press, 1991). Briefly, mitral cell dendrites are much larger in diameter, their cytoplasm is less electrondense, have many mitochondria and contain round shaped synaptic vesicles. In contrast, dendrites of granule cells are smaller, more electron dense and rarely contain synaptic vesicles. The distinction between ETCs and periglomerular cell somata are based on the following: ETC somata are much larger in diameter, they have a larger cytoplasm to nucleus ratio with more organelles (e.g. RER, Golgi apparatus) and their nuclei are more euchromatic.
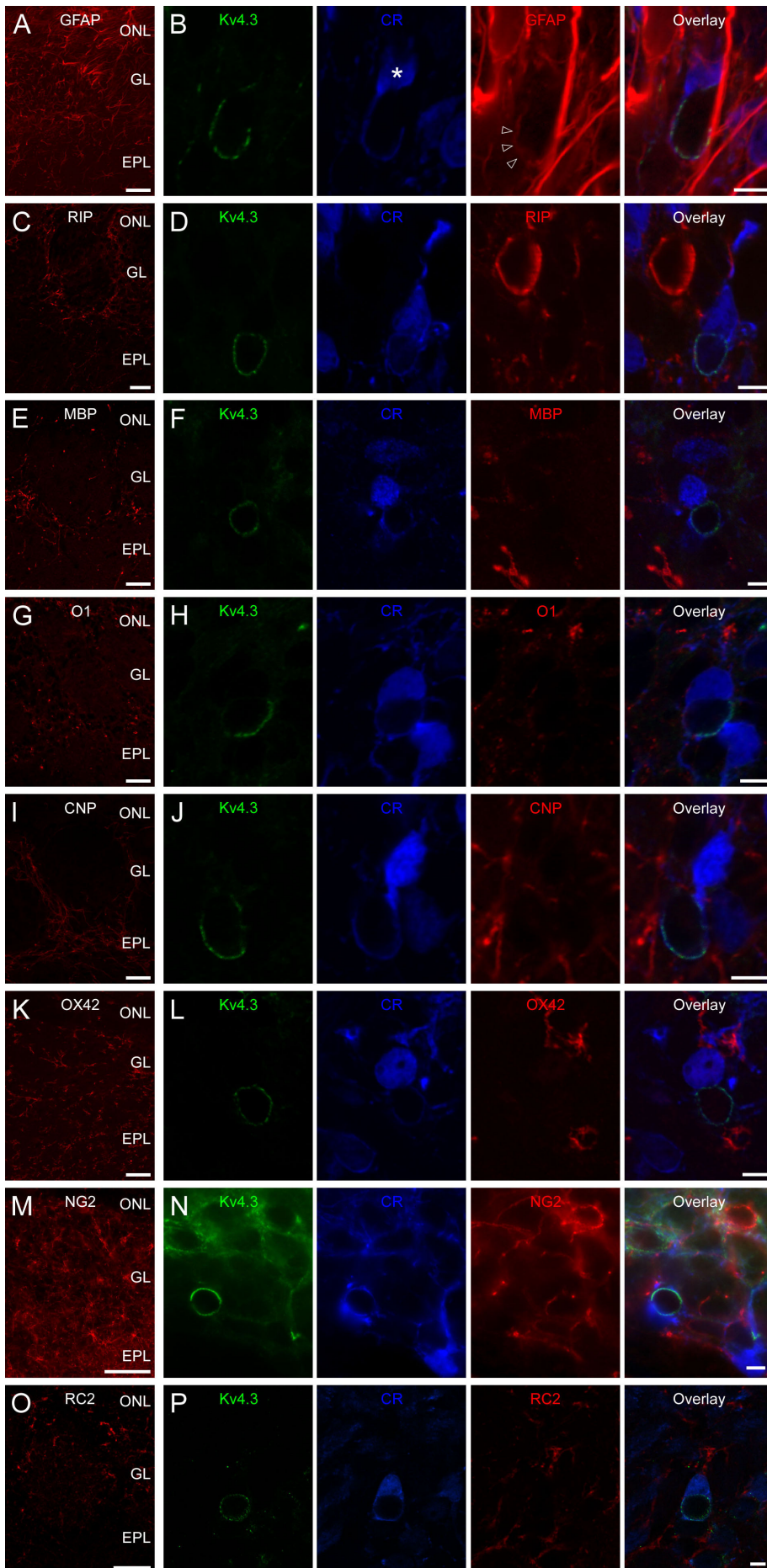
Expression of marker proteins for various glia cell types in the glomerular layer of the MOB. Low magnification views of GFAP (A), RIP (C), MBP (E), O1 (G), CNPase (I), OX42 (K) NG2 (M) and RC2 (O) immunoreactivity in the external plexiform (EPL), glomerular (GL) and olfactory nerve (ONL) layers. B, A weakly GFAP immunopositive process (arrowheads) surrounds a Kv4.3 subunit positive cap formed by a calretinin (CR) positive cell (*). GFAP labeling is absent from the CR+ soma and the proximal part of the neurit. Calretinin positive cells forming Kv4.3 subunit immunolabeled caps are immunonegative for oligodendrocyte marker proteins RIP (D), MBP (F), O1 (H) and CNPase (J), the microglia marker OX42 (L), the oligodendrocyte precursor marker NG2 (N) and the radial glia marker RC2 (P). Single confocal sections are shown. Scale bars: A, C, E, G, I, K, M, O: 40 μm; B, D, F, H, J, L, N, P: 5 μm
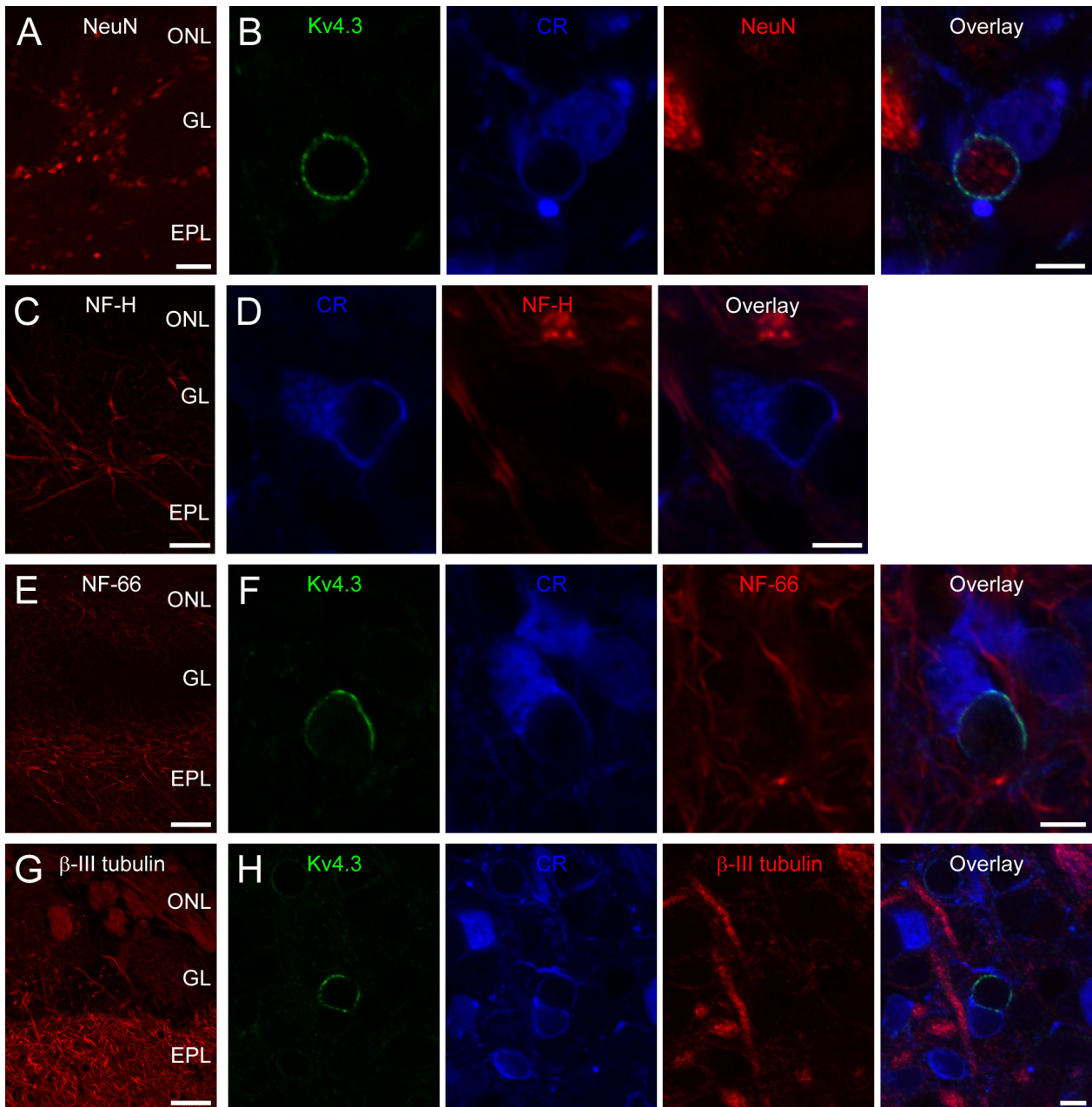
Distribution of immunoreactivity for different marker proteins for neurons in the glomerular layer. Low magnification views of NeuN (A), neurofilament-H (C), Neurofilament α-Internexin/NF66 (E) and β-III tubulin (G) immunoreactivity in the external plexiform (EPL), glomerular (GL) and olfactory nerve (ONL) layers. B, D, F, H, Calretinin positive cells forming Kv4.3 subunit immunolabeled caps are immunonegative for all of these markers. Single confocal sections are shown. Scale bars: A, C, E, G: 40 μm; B, D, F, H: 5 μm
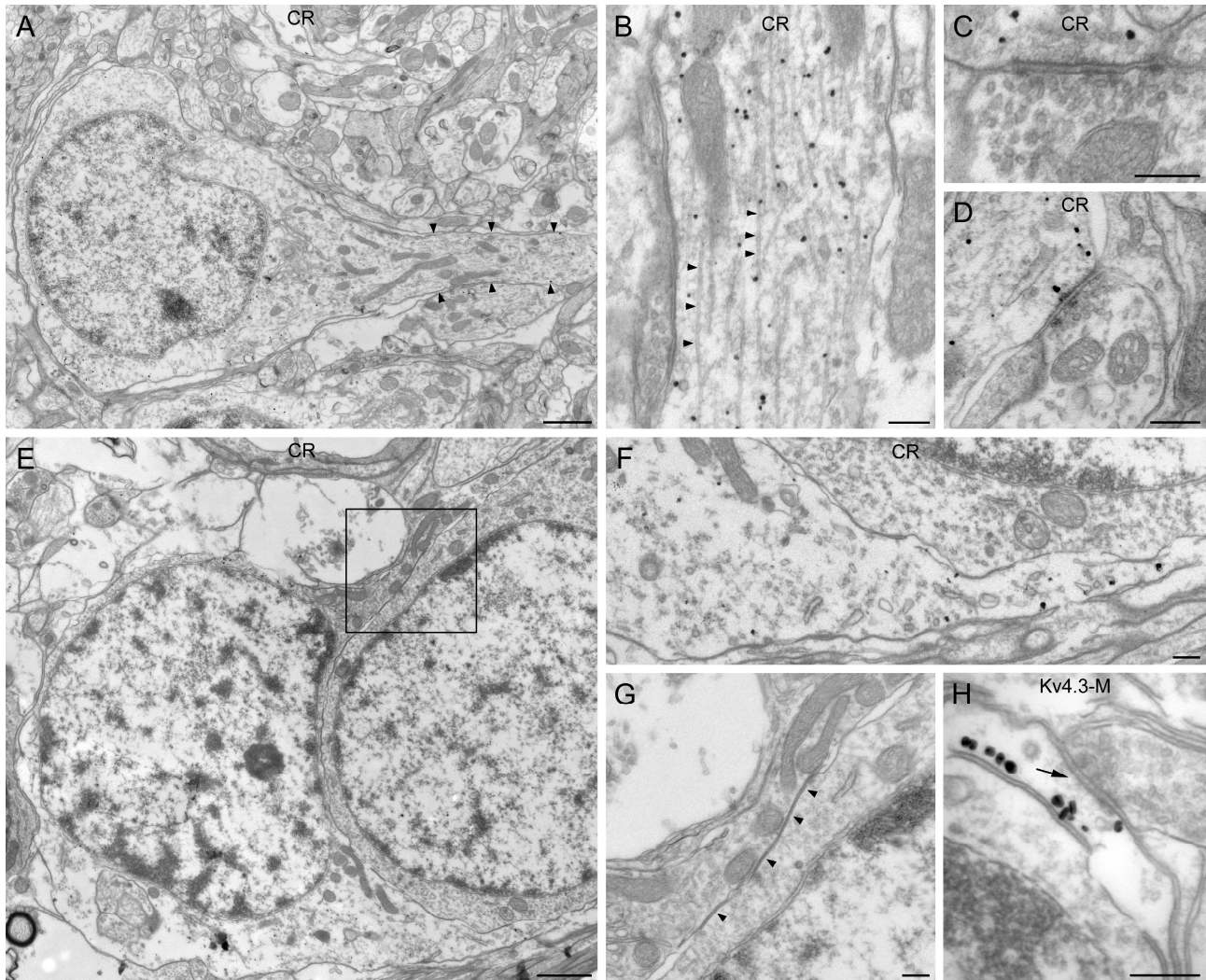
Distinct ultrastructural features of calretinin immunopositive (CR+) juxtaglomerular cells. A, A typical CR+ PGC possesses a single dendrite (arrowheads) that enters the glomerulus. B, A proximal dendrite of a typical CR+ PGC contains many microtubules (arrowheads). C, D, Branches are formed mostly deep in the glomerulus where the dendrites receive synapses. E, A CR+ juxtaglomerular cell ensheaths the soma of a PGC with its processes. F, A higher magnification image of the bottom right hand side corner of panel E from a serial section showing a large number of gold particles labeling CR. G, A high magnification image of the boxed area on E. The process lacks microtubules and establishes specialized membrane junctions with the surrounded cell (arrowheads). H, Despite the glia-like appearance of these processes, occasionally synaptic specializations (arrow) were found on the perisomatic caps. Note the high density of immunogold

particles labeling the Kv4.3 subunit on the membrane of the perisomatic cap that touches the PGC

soma.   Scale bars: A, E, 1 µm; B-D, F-H, 0.2 µm
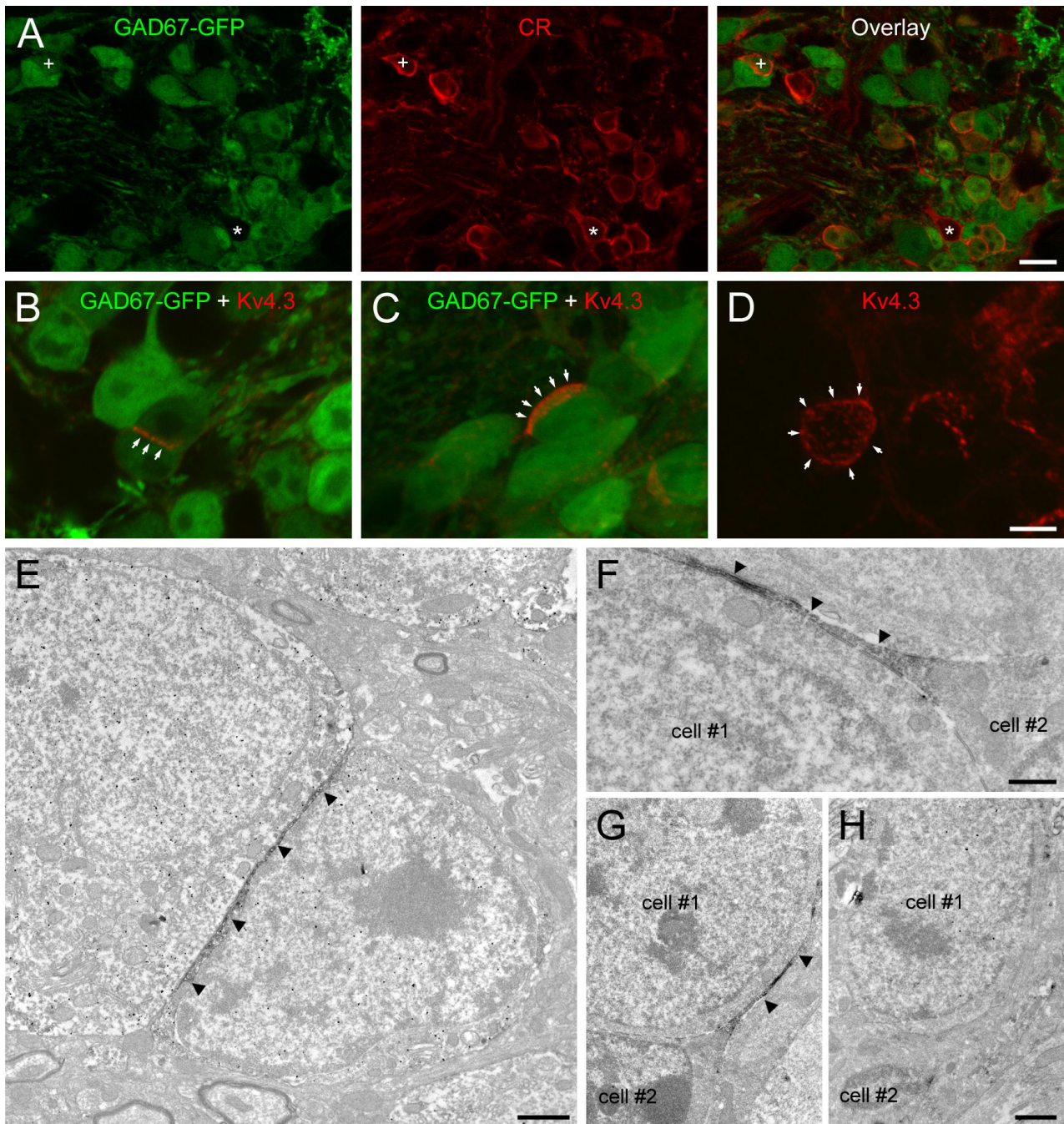
Distribution of the Kv4.3 subunit in the glomerular layer of GAD67-GFP knock-in mice. (A) The majority of the CR immunopositive periglomerular cells express GFP (e.g. +), but 6.3±1.2% of the CR-immunopositive cells are GFP-negative (e.g. *). Single confocal sections are shown. (B) In mice, Kv4.3 subunit immunopositive clusters (arrows) were frequently found between the somata of GFP expressing periglomerular neurons. Kv4.3 subunit immunopositive perisomatic cap-like structures were also found (arrows; maximum intensity projection image of 14 confocal sections), but these were less frequent and covered a smaller portion of the surrounded cells somata in mice

compared to corresponding structures in rats (D, arrows; maximum intensity projection image of 14 confocal sections). (E) Electron micrograph showing two GFP expressing periglomerular neurons (gold particles label GFP). Strong Kv4.3 subunit labeling (DAB reaction end-product, arrowheads) is present at the plasma membrane of one of the cells where the two cells are in direct contact. (F) A thin process of a juxtaglomerular cell (cell #2) surrounds the cell body of another cell (cell #1) with a thin, Kv4.3 subunit immunopositive process (DAB reaction end-product, arrowheads). The same cells are shown at lower magnification on (G). The same two cells are shown on a more superficial section (H), where the anti-GFP immunogold reaction is prominent. The cell surrounded by the thin process (cell #1) contains gold particles labeling GFP. The cap-forming cell is GFP immunonegative. Scale bars: A: 10 μm; B, C, D: 5 μm; E, G, H: 1 μm; F: 0.2 μm

| Biocytin | Kv4.3 | CR | Overlay |
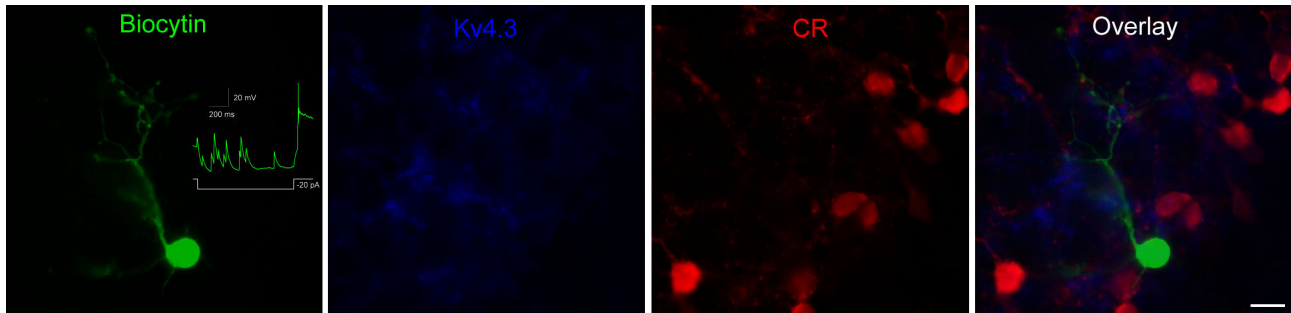
Morphological, neurochemical and electrophysiological characterization of an *in vitro* whole-cell patch-clamp recorded periglomerular cell. The voltage response to -20 pA current injection of the PG cell is shown in the inset. Note the large amplitude, spontaneously occuring EPSPs. At the end of the DC current injection, the cell fired a rebound action potential. Following the recordings, the intracellularly applied biocytin was visualized (green) and immunoreaction for the Kv4.3 subunit (blue) and for calretinin (red) was carried out on the sections. The biocytin-filled cell is immunonegative both for calretinin and Kv4.3. Scale bar: 10 µm.

Suppl. Table. 1.

Description of primary antibodies used in the present study

Antibody	Source	Location	Cat.No.	Host	Epitope or immunogen	Dilution
Kv4.2-M	NeuroMab	UC Davis/NINDS/NIMH	75-016	Mouse	209-225	1:500-1:1000
Kv4.2-R	Alomone	Jerusalem, Israel	APC-023	Rabbit	454-469	1:500
Kv4.3-M	NeuroMab	UC Davis/NINDS/NIMH	75-017	Mouse	415-636	1:500-1:1000
Kv4.3-R	Chemicon	Temecula, CA	AB5194	Rabbit	451-467	1:200-1:500
Kv4.3-G	Santa-Cruz	Santa Cruz, CA	sc-11686	Goat	a short epitope between 470-550	1:100-1:250
CR	Swant	Bellinzona, Switzerland	6B3	Mouse	50-85	1:1000
CR	Oncogene	Cambridge, MA	PC-254L	Rabbit	chick CR fusion protein	1:1000
PV	Swant	Bellinzona, Switzerland	PV-28	Rabbit	rat muscle parvalbumin	1:1000
vGluT2	Synaptic Systems	Goettingen, Germany	135 102	Rabbit	510-582	1:500
NeuN	Chemicon	Temecula, CA	MAB377	Mouse	purified cell nuclei from mouse brain	1:1000
Tubulin βIII TU-20	Chemicon	Temecula, CA	MAB1637	Mouse	443-450	1:1000
Neuro-filament 200 NF-H	Sigma	Saint Louis, MO	N0142	Mouse	C-terminal segment of enzymatically dephosphorylated pig neurofilament 200	1:250
Neuro-filament α internexin NF66	Imgenex	San Diego, CA	IMG-5071A-2	Rabbit	Purified bovine NF66	1:100
GFAP	Sigma	Saint Louis, MO	G3893	Mouse	GFAP from pig spinal cord	1:1000
RIP	DSHB	Iowa City, IA	RIP	Mouse	rat olfactory bulb	1:1000
CD11b	Chemicon	Temecula, CA	CBL1512	Mouse	rat peritoneal macrophages	1:500
CNP	Boehringer Mannheim	Mannheim, Germany	1442 007	Mouse	2$0$,3$0$-cyclic nucleotide 3$0$-phosphodiesterase	1:100
NG2	Chemicon	Temecula, CA	MAB5384	Mouse	Cell line expressing a truncated form of NG2	1:50
RC2	DSHB	Iowa City, IA	RC2	Mouse	rat fetal brain	1:500
GABA	Szabat et al., 1992			Mouse	BSA conjugated GABA with glutaraldehyde	1:50
GFP	Chemicon	Temecula, CA	AB3080P	Rabbit	Highly purified native GFP from Aequorea victoria	1:500
MBP	Espinosa de los Monteros et al., 1988			Mouse		1:100
O1	Espinosa de los Monteros et al., 1988			Mouse		1:100